

Towards Learning and Explaining Indirect Causal Effects in Neural Networks

Abbavaram Gowtham Reddy¹, Saketh Bachu¹, Harsharaj Pathak¹, Benin L. Godfrey¹,
Varshaneya V², Vineeth N. Balasubramanian¹, Satyanarayan Kar²

¹ Indian Institute of Technology Hyderabad, India

² Honeywell, Bengaluru, India

Abstract

Recently, there has been a growing interest in learning and explaining causal effects within Neural Network (NN) models. By virtue of NN architectures, previous approaches consider only direct and total causal effects assuming independence among input variables. We view an NN as a structural causal model (SCM) and extend our focus to include indirect causal effects by introducing feedforward connections among input neurons. We propose an ante-hoc method that captures and maintains direct, indirect, and total causal effects during NN model training. We also propose an algorithm for quantifying learned causal effects in an NN model and efficient approximation strategies for quantifying causal effects in high-dimensional data. Extensive experiments conducted on synthetic and real-world datasets demonstrate that the causal effects learned by our ante-hoc method better approximate the ground truth effects compared to existing methods.

1 Introduction

Neural network (NN) models enriched with causal knowledge have demonstrated their ability to achieve robustness [36], invariance [27, 9], and provide interpretable explanations for human understanding [3, 26, 17]. In training such NN models imbued with causal knowledge, two primary tasks emerge: (1) acquiring a comprehension of causal relationships between input and output neurons [15, 21, 17], and (2) validating and explaining the acquired causal relationships [3, 16, 26]. Previous studies have tended to address these two tasks separately, despite their close interconnectedness. This separation of dependent tasks also makes it challenging to study and model more nuanced aspects such as the indirect causal effects of input neurons on the output of an NN. To address this limitation, in this work, we propose an Ante-Hoc Causal Explanations (AHCE) approach that simultaneously performs both these tasks.

Task 1 - Learning Causal Effects in NNs: A common practice in learning causal effects in NN models involves considering the NN as a Structural Causal Model (SCM), representing the parametric causal relationships between the features [19, 3, 16]. Given our focus on input-output causal relationships in an NN, following [19, 3, 17], we marginalize

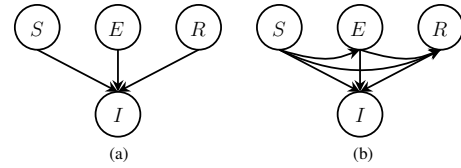


Figure 1: (a) A marginalized NN whose inputs S, E, R are not causally related. (b) A marginalized NN whose inputs are connected through feedforward connections (e.g., $S \rightarrow E$) to capture underlying causal relationships (e.g., S causes E) to learn the indirect causal effects of inputs on output (e.g. effect of S on I via E).

the hidden layers and view the output as a function of inputs as shown in Fig 1 (a) (the motivating example in the next paragraph describes the variables). It becomes evident that the SCM embodied by a conventional feedforward NN model lacks causal relationships among input features (neurons in the first layer, we use *input features* and *input neurons* interchangeably in this work). Consequently, the causal effects that are learned and quantified are restricted solely to *direct causal effects* (*viz.* causal effects that do not propagate through other input features – see Appendix §A for preliminaries). Hence, there is currently no feasible approach for explaining *indirect causal effects* (*viz.* causal effects that propagate through other input features). We extend the basic architecture of an NN by adding feedforward connections among input neurons (see Fig 1(b)) based on domain knowledge of how features interact in the real-world, thus enabling the learning and explaining of indirect causal effects.

To motivate the need for the study of indirect causal effects in NN models, consider the task of predicting an individual’s income (I) using the features: education (E), socioeconomic status (S), and job role (R). In the real world, S causes E and R ; E causes R ; S, E , and R cause I (see Fig 1(b)). However, in an NN model, the relationships among input features S, E, R are not modeled (see Fig 1(a)). As a result, for feature S , an NN model can only learn and explain direct causal effects while neglecting the indirect causal effects on I propagating via E and R . From a fairness standpoint, S should have no direct causal effect on I but can exhibit a non-zero indirect causal effect on I through E and R . If a model learns a non-zero direct causal effect of S on I , the corresponding model explanations may not align

Method	Direct Effects	Indirect Effects	Total Effects	Causal Effects	Ante-hoc Explanations
IG [S 2017]	✓	✗	✗	✗	✗
CA [AC 2019]	✓	✗	✗	✓	✗
CSHAP [TH 2020]	✓	✓	✓	✗	✓
CREDO [SK 2022]	✓	✗	✓	✓	✓
AHCE (Ours)	✓	✓	✓	✓	✓

Table 1: Comparison of various explanation methods. IG refers to Integrated Gradients and CA refers to Causal Attributions.

with the real-world and can indicate unacceptable learned causal effects. Thus, learning indirect effects can also find application in identifying and comprehending model biases. We provide the ability to differentiate between direct and indirect causal effects in an NN model by introducing feedforward connections among input features (see Appendix §H for another motivating example).

Task 2 - Explaining Causal Effects in NNs: Explainability methods for NN models have encompassed a wide range of techniques ranging from various gradient-based methods to Shapley values. Recently, there has been increased attention towards causal explanations due to their enhanced reliability [48, 12], as well as their potential for aiding in debugging [8] and improving NN model performance [21, 17]. We refer to explanations such as gradients and Shapley values as *effects* and causal explanations as *causal effects* to separate the non-causal explanations from causal explanations. Most explanation methods provide direct effects, such as gradients and marginal Shapley values [22]. Causal Shapley values (CSHAP) [13] account for indirect effects mediated through other features. However, they are not equal to the causal effects obtained through backdoor adjustment [30] (see Appendix §B for details). Except for causal regularization using domain priors (CREDO) [17], all existing efforts in causal explanations are post-hoc approaches, quantifying the causal effects of input features on the output for a pre-trained NN model. These post-hoc explanation methods, though causal, only capture direct effects, and assign zero indirect causal effects to all features. This may not accurately represent the true underlying indirect causal effects among input features in the real world [16]. Although [17] adopts an ante-hoc approach, it does not model indirect causal effects. See Tab 1 for a comparison of related explanation methods. To the best of our knowledge, this is the first work that provides an ante-hoc approach to explain indirect causal effects. Our key contributions are summarized below.

- We propose a novel ante-hoc training algorithm to capture indirect causal effects in NN models. Our approach aligns with the demand for intrinsically interpretable techniques rather than post-hoc explanations [34].
- We propose an algorithm to quantify the learned indirect causal effects in NNs using the lateral connections among input neurons.
- We also present effective implementation strategies to scale causal explanation methods to high-dimensional data w.r.t. time and space complexity.
- We present a wide range of empirical results on both synthetic and real-world datasets to showcase the usefulness

of the proposed method.

2 Related Work

Learning Structural Causal Models: Learning the structural causal model (SCM) is a core component of tasks in causal inference, including causal effect estimation [52], and counterfactual generation [28]. In a work possibly closest to our work, [52] propose the learning of neural causal models (NCM) utilizing the underlying causal graph as an inductive bias, with a specific emphasis on identifying and learning ground truth causal effects. However, our objective in this effort is different from NCM; our focus lies in the causal effects pertaining to an NN model, primarily designed to enhance predictive accuracy. Our methodology remains applicable even when only partial knowledge of the underlying causal graph is accessible.

Explainability: In addition to promoting transparency in decision-making processes, the elucidation of NN models serves several purposes, including the identification of concealed biases present in data [1], the revelation of fairness [6], the debugging [8] and enhancement of models through explanation-based regularizers [33, 32, 17]. Numerous existing methods for explaining NN models quantify the impact of input features on model outputs using saliency maps [55, 42, 40], local model approximations [31], approximations of output gradients with respect to inputs [44, 43], Shapley values [22, 13], among others. In this work, we focus on the causal effects of input features on output in an NN model, which can be very useful in safety-critical domains such as healthcare, aerospace, law, and defense. See Appendix §I to understand further why causal explanations are important through a real-world example.

Causal Explanations: By considering an NN as an SCM, assuming that input features are d -separated from each other, [3] proposed a post-hoc causal explanation method to find the average causal effects (ACE) in a trained NN. However, the assumption of independence among inputs limits their ability to consider indirect causal effects. Subsequent studies by [18, 53, 49, 37, 10] have followed ACE as defined therein to quantify the learned causal effects. Other causal explanation methods utilize counterfactuals to analyze model behavior under semantically meaningful changes applied to inputs [46, 11, 48, 4, 45, 25, 23]. However, these methods are commonly employed for qualitative analysis of the model rather than computing causal effects.

Direct and Indirect Explanations: Among existing efforts that explicitly investigate interactions among input variables while computing explanations for NN models, prominent methods are those based on Shapley values [22]. For instance, in the context of handling missing features in Shapley explanations, it is discouraged to sample from the conditional distribution (rather than the marginal distribution) because the inputs are independent with respect to the causal graph of the NN [16]. While [13] considers both direct and indirect effects motivated by the direct and indirect pathways in the underlying causal graph, even if input neurons of the NN model being explained do not have causal connections, its focus is on providing Shapley values that may not necessarily be causal effects obtained from the adjustment

formula (see Appendix §B). In this study, we consider input feature interactions while learning and explaining causal effects in NNs. Our approach explicitly estimates and preserves indirect causal effects in an NN model. While [17] discusses direct and total causal effects for NN model explanations, it does not focus on indirect causal effects. The work most closely related to ours is presented in [47], which examined both direct and indirect causal effects in Transformer-based language models for capturing gender bias. However, that study conducted a post-hoc analysis of such models for a different objective, whereas our proposed method represents an ante-hoc approach to learning and explaining both direct and indirect causal effects. Other related work, such as concept-based explanation methods, are discussed in Appendix §G.

3 Causal Effects in Neural Networks

Let $\mathcal{G} = (\mathbf{V}, \mathbf{E})$ be a causal graph where $\mathbf{V} = \{X_1, X_2, \dots, X_n, Y\}$ is the set of random variables and \mathbf{E} is the set of edges denoting the causal influences among the variables in \mathbf{V} . Let $\mathbf{X} = \{X_1, \dots, X_n\} = \mathbf{V} \setminus \{Y\}$, $ch(X_i) = \{X_j | X_i \rightarrow X_j\} \subseteq \mathbf{V} \setminus \{X_i, Y\}$ be the set of children of X_i except Y , and $pa(X_i) = \{X_j | X_i \leftarrow X_j\} \subseteq \mathbf{V} \setminus \{X_i, Y\}$ be the set of parents of X_i except Y . This definition of $ch(X_i)$ and $pa(X_i)$ allows us to model indirect effects between input variables. Let \mathcal{N} be an NN model that is trained to predict Y given \mathbf{X} as input by minimizing the empirical loss \mathcal{R}_{ERM} in Eq 1 for a given set $D = \{(x_1^j, \dots, x_n^j, y^j)\}_{j=1}^N$ of N data points.

$$\mathcal{R}_{ERM} = \frac{1}{N} \sum_{j=1}^N \mathcal{L}(y^j, \mathcal{N}(x_1^j, \dots, x_n^j)) \quad (1)$$

where \mathcal{L} is an appropriate loss function such as root mean squared error for regression and cross-entropy loss for classification. Let $\hat{Y} = \mathcal{N}(X_1, \dots, X_n)$ be the overall output of the final layer of \mathcal{N} . \mathcal{N} can be conceptualized as a directed acyclic graph (DAG) comprising directed edges connecting successive layers of neurons. Consequently, the output \hat{Y} can be understood as the outcome arising from a series of interactions from the first to the final layer. When studying the causal effects of inputs on the output of \mathcal{N} , solely the neurons in the first and final layers are considered. Consequently, similar to [3], we can marginalize the influence of hidden layers within \mathcal{N} and focus solely on the causal structure involving inputs and outputs (see Fig 1 (a)). Note that while we follow [3] in our view of NN as an SCM, they do not consider or model indirect effects, which is the focus of our work. To this end, we begin by defining various causal effects of input features on the output of a trained NN model.

Definition 3.1. (Average Causal Effect in an NN) *The Average Causal Effect (ACE) of an input feature X_i at an intervention x_i with respect to a baseline intervention x_i^* on the output \hat{Y} of an NN \mathcal{N} is defined as*

$$ACE_{X_i}^{\hat{Y}} = \mathbb{E}[\hat{Y} | do(X_i = x_i)] - \mathbb{E}[\hat{Y} | do(X_i = x_i^*)]$$

where $do(X_i = x_i)$ denotes an external intervention to the variable X_i with the value x_i (see Defn. A.3 in Appendix

A). We use $do(X_i)$ to refer to $do(X_i = x_i)$ when there is no ambiguity. *ACE* is also called the average total causal effect, which is the sum of direct and indirect causal effects.

Definition 3.2. (Average Direct Causal Effect in an NN) *The Average Direct Causal Effect (ADCE) measures the causal effect of a feature X_i on the output \hat{Y} of an NN when $\mathbf{Z} = ch(X_i)$ are intervened with values under the baseline intervention $do(X_i = x_i^*)$, denoted by $\mathbf{Z}_{X_i^*}$.*

$$ADCE_{X_i}^{\hat{Y}} = \mathbb{E}[\hat{Y} | do(X_i, \mathbf{Z}_{X_i^*})] - \mathbb{E}[\hat{Y} | do(X_i^*, \mathbf{Z}_{X_i^*})]$$

Definition 3.3. (Average Indirect Causal Effect in an NN) *The Average Indirect Causal Effect (AICE) measures the causal effect of a feature X_i on the output \hat{Y} of an NN when $\mathbf{Z} = ch(X_i)$ are intervened with values under $do(X_i = x_i)$, denoted by \mathbf{Z}_{X_i} , while keeping the X_i value fixed at the baseline intervention $do(X_i = x_i^*)$.*

$$AICE_{X_i}^{\hat{Y}} = \mathbb{E}[\hat{Y} | do(X_i^*, \mathbf{Z}_{X_i})] - \mathbb{E}[\hat{Y} | do(X_i^*, \mathbf{Z}_{X_i^*})]$$

4 Learning and Explaining Direct and Indirect Causal Effects in Neural Networks

We now present our methodology for learning and explaining indirect causal effects within NNs. Following [41, 38, 56], we make the following assumption concerning the underlying causal graph \mathcal{G} .

Assumption 4.1. *There are no latent (unobserved) confounders in the underlying causal graph \mathcal{G} .*

To quantify direct and indirect causal effects of an input X_i on the output \hat{Y} of an NN, it is required to perform an intervention on $ch(X_i)$ with specific values based on X_i 's value (as formally stated in Defns 3.2 and 3.3). The above assumption allows us to get the values to perform an intervention on $ch(X_i)$.

Hypothesis 4.1. *In an NN \mathcal{N} , the indirect effect of a variable X_i on Y via $ch(X_i)$, $AICE_{X_i}^{\hat{Y}}$, is identifiable in \mathcal{N} iff there are feedforward edges from X_i to $ch(X_i)$ in the architecture of \mathcal{N} .*

The supporting proof for the above hypothesis is straightforward and provided in Appendix §C. Note that the edges between X_i and $ch(X_i)$ capture the true causal relationships in the real-world. In such an architecture of \mathcal{N} with lateral edges between X_i and $ch(X_i)$, the weights parametrizing these edges are also learned by \mathcal{N} along with other weights in the model while optimizing for \mathcal{N} 's objective.

Although Hypothesis 4.1 may appear self-evident, it has been overlooked in existing methods for explaining NN models. For example, [16] argue that *Shapley* explanations in a simple feedforward NN should treat all input features to be independent because the causal graph of a simple feedforward NN has no causal connections among input neurons. A similar argument is given by [5] focusing on only *direct* effects while quantifying input influence on the output of an NN. Not accounting for indirect effects when modeling statistical relationships in the observed data distribution (e.g., using conditional expectation instead of marginal expectation for missing features while calculating Shapley values) may generate incorrect explanations [16].

4.1 Learning Indirect Causal Effects

Following the above discussion, given a standard NN \mathcal{N} , we propose an augmented NN architecture \mathcal{N}^{Ind} for capturing indirect causal effects of input features on the output. \mathcal{N}^{Ind} contains lateral directed connections among the input neurons based on the available knowledge of the true causal graph (see Fig 2). Our methodology remains applicable even when only a partial causal graph is available, capturing indirect effects exclusively on the available connections. We call the set of NN edges introduced among input neurons as layer 0 connections to separate them from NN connections in hidden layers. These connections among input features have learnable parameters akin to other parameters within the NN.

Algorithm 1: Pseudocode for training \mathcal{N}^{Ind} model

```

1: Input: True causal graph  $\mathcal{G}$ ,  $\mathcal{D} = \{(x_1^j, \dots, x_n^j, y^j)\}_{j=1}^N$ , parameters  $\theta_0, \dots, \theta_m$  of layers  $l_0, \dots, l_m$  of  $\mathcal{N}^{Ind}$ ,  $\lambda$ , functions  $f_i^0$  in  $l_0$  learned by introducing edges among input features.
2: Output: Trained  $\mathcal{N}^{Ind}$  model
3: for each epoch do
4:   for phase in [1, 2] do
5:     if phase = 1 then
6:        $\mathcal{R}_{ERM} = \frac{1}{N} \sum_{j=1}^N \mathcal{L}(y^j, \mathcal{N}^{Ind}(x_1^j, \dots, x_n^j))$ 
7:       Compute gradients of  $\mathcal{R}_{ERM}$  w.r.t.  $\theta_1, \dots, \theta_m$ 
8:       Update the parameters  $\theta_1, \dots, \theta_m$  using SGD
9:     else
10:      for each  $(x_1^j, \dots, x_n^j, y^j)$  in  $\mathcal{D}$  do
11:         $x_i^j = f_i^0(pa(x_i^j)) \forall i \text{ s.t. } pa(X_i) \neq \emptyset$ 
12:      end for
13:       $\mathcal{R} = \mathcal{R}_{ERM} + \lambda \sum_{j=1}^N \sum_{\{i | pa(X_i) \neq \emptyset\}} (x_i^j - f_i^0(pa(x_i^j)))^2$ 
14:      Compute gradients of  $\mathcal{R}$  w.r.t.  $\theta_0, \dots, \theta_m$ 
15:      Update parameters of  $\theta_0, \dots, \theta_m$  using SGD
16:    end if
17:  end for
18: end for
19: return trained  $\mathcal{N}^{Ind}$ 

```

To train the augmented \mathcal{N}^{Ind} model, we propose an ante-hoc training algorithm consisting of two phases, each of which is invoked sequentially in each epoch. In the first phase, we freeze the parameters of the layer 0 and train the remaining part of the NN. In the second phase, we train the entire model i.e., parameters of layer 0 to the final layer. In the second phase, the input to the \mathcal{N}^{Ind} model is constructed as follows. Consider a specific input data point $(x_1^j, \dots, x_n^j) \sim \mathcal{D}$. The value of each input variable X_i for which $pa(X_i) = \emptyset$ is taken from (x_1^j, \dots, x_n^j) , and the remaining input feature values are *derived topologically* by feeding the other input variables into layer 0. That is, for each X_i with $pa(X_i) \neq \emptyset$, if f_i^0 is the function of its parents $pa(X_i)$ in layer 0, we derive $X_i = f_i^0(pa(X_i))$. Please note that f_i^0 is modeled by the NN connections in layer 0. These two training phases are carried out sequentially in every epoch until we reach the desired minimum loss value (or appropriate stopping condition). To aid better learning of

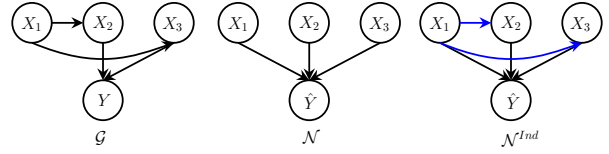


Figure 2: Comparison of the proposed architecture \mathcal{N}^{Ind} with a traditional NN architecture \mathcal{N} . \mathcal{G} is the ground truth causal graph. \mathcal{N} and \mathcal{N}^{Ind} differ in input layer such that the inputs in \mathcal{N}^{Ind} are connected (shown in blue color) according to the causal edges in \mathcal{G} . In contrast, the inputs in \mathcal{N} are independent. \mathcal{N} and \mathcal{N}^{Ind} may contain edges that are not present in \mathcal{G} due to the feedforward connections from input layer to predictions in NN architecture (e.g., $X_1 \rightarrow \hat{Y}$ is present in \mathcal{N} , \mathcal{N}^{Ind} but not in \mathcal{G}).

parameters of layer 0, we add a regularization term to the empirical loss \mathcal{R}_{ERM} in Eqn 1 that incurs a penalty if the derived feature values deviate from actual feature values in the training data. Eqn 2 shows the overall loss value used in phase 2 with regularization term and corresponding regularization hyperparameter λ . \mathcal{N}^{Ind} is trained using stochastic gradient descent (SGD), as with any other NN model. Algorithm 1 summarizes this training procedure.

$$\mathcal{R} = \mathcal{R}_{ERM} + \lambda \sum_{j=1}^N \sum_{\{i | pa(X_i) \neq \emptyset\}} (x_i^j - f_i^0(pa(x_i^j)))^2 \quad (2)$$

4.2 Explaining Indirect Causal Effects

On training the ante-hoc model \mathcal{N}^{Ind} , we now present a methodology to compute the acquired indirect causal effects in the learned model. We begin by formally defining causal effect *identifiability* in this context.

Definition 4.1. Causal Effect Identifiability in an NN. *The causal effect of an input feature X_i on the output \hat{Y} of an NN is identifiable if $p(\hat{Y}|do(X_i))$ can be computed uniquely from any positive probability distribution $p(X_1, \dots, X_n, \hat{Y})$.*

Under the *no latent confounding* assumption (Assumption 4.1), following Theorem 3.2.5 and Corollary 3.2.6 of [30], it is easy to show that $ADCE_{X_i}^{\hat{Y}}$ and $AICE_{X_i}^{\hat{Y}}$ are identifiable in \mathcal{N}^{Ind} (we provide formal proofs in Appendix §C). Now, to evaluate $ADCE_{X_i}^{\hat{Y}}$ and $AICE_{X_i}^{\hat{Y}}$ in \mathcal{N}^{Ind} , we need to in turn evaluate the following quantities: $\mathbb{E}[\hat{Y}|do(X_i^*, \mathbf{Z}_{X_i^*})]$, $\mathbb{E}[\hat{Y}|do(X_i, \mathbf{Z}_{X_i^*})]$ and $\mathbb{E}[\hat{Y}|do(X_i^*, \mathbf{Z}_{X_i})]$ (see Defns 3.2, 3.3 and recall that $\mathbf{Z} = ch(X_i)$). These terms, which are of the form $\mathbb{E}[\hat{Y}|do(\mathbf{S})]$ where \mathbf{S} is a set of features, often require us to marginalize over other input features $\mathbf{X} \setminus \mathbf{S}$ as:

$$\mathbb{E}[\hat{Y}|do(\mathbf{S})] = \mathbb{E}_{\mathbf{X} \setminus \mathbf{S}} [\mathbb{E}[\hat{Y}|\mathbf{S}, \mathbf{X} \setminus \mathbf{S}]] \quad (3)$$

Evaluating the above expression, typically using an *adjustment set* (see Defn A.4 in Appendix §A), can incur significant computational overhead, which grows exponentially with the number of features in $\mathbf{X} \setminus \mathbf{S}$, especially when they

are continuous and real-valued. To avoid such prohibitive computational requirements, following earlier work [24, 3], we consider the second-order Taylor’s approximation to the NN output $\hat{Y} = f(\mathbf{X})$ around the mean vector μ , where $\mu_j = \mathbb{E}[X_j|do(\mathbf{S})]$ as follows:

$$f(\mathbf{X}) \approx f(\mu) + \nabla^T f(\mu)(\mathbf{X} - \mu) + \frac{1}{2}(\mathbf{X} - \mu)^T \nabla^2 f(\mu)(\mathbf{X} - \mu)$$

Taking interventional expectations on both sides gives:

$$\mathbb{E}[f(\mathbf{X})|do(\mathbf{S})] \approx f(\mu) + \frac{1}{2}Tr(\nabla^2 f(\mu)\mathbb{E}[(\mathbf{X} - \mu)(\mathbf{X} - \mu)^T|do(\mathbf{S})]) \quad (4)$$

The first-order terms vanish because $\mathbb{E}[\mathbf{X}|do(\mathbf{S})] = \mu$. To evaluate Eqn 4, we need to calculate the interventional mean vector $\mu = \mathbb{E}[\mathbf{X}|do(\mathbf{S})]$ and the interventional covariance matrix $\mathbb{E}[(\mathbf{X} - \mu)(\mathbf{X} - \mu)^T|do(\mathbf{S})]$.

We present the following steps $S1 - S4$ to evaluate interventional means and covariances for interventions: $do(X_i^*, \mathbf{Z}_{X_i^*})$, $do(X_i, \mathbf{Z}_{X_i^*})$, and $do(X_i^*, \mathbf{Z}_{X_i})$.

- S1. For an intervention on X_i with the value x_i , set $\mu[i] = x_i$.
- S2. To get interventional values \mathbf{Z}_{X_i} for the variables in \mathbf{Z} under the intervention $do(X_i = x_i)$, for each variable $X_p \in \mathbf{Z}$ taken in topological order, compute $X_p = f_0^p(pa(X_p))$ and $\mu[p] = \mathbb{E}_{pa(X_p)}[\mathbb{E}[X_p|X_i, pa(X_p) \setminus \{X_i\}]]$. This step accounts for updating the values of children of X_i based on the intervention on X_i .
- S3. For each variable $X_q \notin \mathbf{Z}$, set $\mu[q] = \mathbb{E}[X_q]$.
- S4. Compute the interventional covariance matrix from the interventional data distribution obtained after performing step S2.

After performing the above steps, we can substitute the interventional mean and covariance matrix in Eqn 4 to evaluate the expressions $\mathbb{E}[\hat{Y}|do(X_i^*, \mathbf{Z}_{X_i^*})]$, $\mathbb{E}[\hat{Y}|do(X_i, \mathbf{Z}_{X_i^*})]$, $\mathbb{E}[\hat{Y}|do(X_i^*, \mathbf{Z}_{X_i})]$. An algorithm summarizing this overall procedure of evaluating $ADCE_{X_i}^{\hat{Y}}$, $AICE_{X_i}^{\hat{Y}}$ in \mathcal{N}^{Ind} is provided in Appendix § D.

4.3 Efficient Implementation Strategies

Computation of causal effects, in general, can be compute and memory intensive. We hence also provide a few efficient implementation strategies for such computations, which we also incorporate in our experiments. Let each input $X_i \in \mathbf{X}$ assume one of k possible values ($k = 2$ in the binary case). Evaluating causal effects takes roughly $\mathcal{O}(n^k)$ time because of the marginalization step in Eqn 3, where n is the dimensionality of the input vector \mathbf{X} . Evaluating the approximation in Eqn 4 also scales in the order of $\mathcal{O}(n^2)$ as an input intervention may affect all children (Defns 3.2, 3.3). These limitations get accentuated in architectures such as Recurrent Neural Networks (RNNs) (see Appendix F for complexity analysis in RNNs). To address these issues, we propose the following improvements.

Runtime Efficiency using Binning: Computing causal effects using Eqn 4 requires computing the interventional

mean and interventional covariance (interventional statistics). To speed up this calculation, we divide the computation into offline and online phases. In the offline step (which can be done independent of the NN training phase), for every data point \mathbf{X} in the training set, we generate and store the interventional statistics for all features $X_i \in \mathbf{X}$ for all interventional values. In the online phase, to find the causal effect for feature X_i with intervention value of x_i in a test data point \mathbf{X}_{te} , we first find the data point \mathbf{X}_{tr} in the training set that is most similar to \mathbf{X}_{te} . Let α be the value taken by feature X_i in \mathbf{X}_{tr} , closest to x_i . We access the interventional statistics stored for \mathbf{X}_{tr} corresponding to feature X_i with intervention α (computed in the offline phase). This retrieved *nearest* interventional statistics is used for causal effect computation. This procedure, detailed further in Appendix § F, reduces significant runtime leveraging offline computations. We refer to this approach as *binning* since a training sample captures a bin and acts as a proxy for other samples/values in its neighborhood. To further speed up ACE computation, we exploit the fact that the Hessian term $\nabla^2 f$ in Eqn 4 can be approximated using $J^T J$ where J is the Jacobian of the NN model function (using Gauss-Newton Hessian approximation).

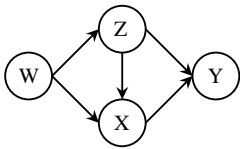
Memory Requirements: Storing offline interventional statistics for every sample on the dataset (and corresponding intervention values) quickly becomes impractical, especially for high-dimensional data. To reduce this memory overhead, we use clustering/hashing techniques (KD Tree, DBSCAN) to cluster training data samples, and store interventional statistics for only cluster centers (see Appendix § F for more details of this strategy). From the results shown in Tab 6, Appendix § F, we observe 3 to 10-fold improvements in run time using the proposed binning approach for a slight reduction in the precision of estimated causal effects.

5 Experiments and Results

We conduct a wide range of experiments across three kinds of datasets – A synthetic dataset, three well-known public real-world benchmark datasets, and three industry-based simulated datasets. We compare the causal explanations of AHCE with a well-known post-hoc gradient-based explanation method: Integrated Gradients (IG) [44], a post-hoc causal explanations (CA) method [3], the causal Shapley values (CSHAP) [13], and a recent causal regularization method in [17]. We compare against IG since it can be viewed as computing individual causal effects of input neurons on the output of an NN [14]. Ground truth causal effects are computed using the adjustment formula in Eqn 3. Following [17], we use the Root Mean Squared Error (RMSE) and Fréchet distance between true causal effects and the learned explanations. We present our results on total causal effects for a fair comparison with all methods (indirect causal effects do not exist for IG, CA, CREDO; comparison of CSHAP with our method on indirect causal effects is presented in Appendix § E). Additional results and experimental setup are presented in Appendix § E owing to space constraints. Our code is provided in the supplementary material.

Synthetic Data: We create a synthetic dataset using a causal

graph and corresponding structural equations shown in Fig 3 and Tab 2. From Fig 3, W has only indirect causal effect on Y via the paths: $W \rightarrow X \rightarrow Y, W \rightarrow Z \rightarrow X \rightarrow Y$, and $W \rightarrow Z \rightarrow Y$. Z has a direct causal effect on Y via the path $Z \rightarrow Y$ and an indirect causal effect on Y via the path $Z \rightarrow X \rightarrow Y$, and X has only a direct causal effect on Y via the path $X \rightarrow Y$. This dataset has linear equations with additive Gaussian noise among input features W, Z, X , and the output Y is a non-linear function of its inputs with additive Gaussian noise. Hence, for purposes of modeling causal effects, the lateral connections among inputs in \mathcal{N}^{Ind} are obtained using simple linear regressors that take a set of real numbers as input and produce a real number as output (for real-world datasets, we replace simple linear regressors with multi-layer perceptrons to account for non-linear relationships among input features).



$$\begin{aligned}
 W &\leftarrow \text{Uniform}(0, 1) \\
 Z &\leftarrow W/2 + \mathcal{N}(0, 0.1) \\
 X &\leftarrow -W - Z + \mathcal{N}(0, 0.1) \\
 Y &\leftarrow X^3 + \log(Z^2) + \mathcal{N}(0, 0.1)
 \end{aligned}$$

Figure 3: Synthetic DAG Table 2: Synthetic Equations

Tab 3 shows the results. The total causal effects given by our method are closer to ground truth causal effects compared to baselines. These results show that the training algorithm for our ante-hoc causal explanation model can better learn both direct and indirect causal effects and match the total causal effects.

We perform an ablation study to empirically verify our hypothesis that adding edges among input features helps in learning causal effects. In this study, we check the causal effects with and without outgoing edges from each input feature W, Z, X in \mathcal{N}^{Ind} (denoted by $\mathcal{N}_{With}^{Ind}, \mathcal{N}_{Without}^{Ind}$ respectively in Tab 4). This setting also resembles real-world scenarios where we can often access only a partial causal graph. From the results in Tab 4, we observe that the total causal effects in \mathcal{N}_{With}^{Ind} are closer to the ground truth total causal effects compared to $\mathcal{N}_{Without}^{Ind}$.

Feature	IG	CA	CSHAP	CREDO	AHCE	
	[S 2017]	[AC 2019]	[TH 2020]	[SK 2022]	(Ours)	
W	0.10±0.00	0.09±0.00	0.24±0.00	0.08±0.01	0.04±0.02	
Z	0.11±0.04	0.04±0.01	0.30±0.00	0.06±0.00	0.05±0.00	
X	0.12±0.00	0.11±0.00	0.25±0.01	0.11±0.00	0.10±0.02	
Average	0.11±0.02	0.08±0.00	0.26±0.00	0.08±0.01	0.06±0.01	
Frechet (↓)	W	0.25±0.00	0.25±0.00	0.25±0.05	0.23±0.03	0.14±0.06
	Z	0.19±0.05	0.09±0.05	0.33±0.02	0.16±0.01	0.13±0.02
	X	0.24±0.07	0.23±0.04	0.32±0.04	0.26±0.03	0.24±0.03
	Average	0.23±0.04	0.19±0.03	0.30±0.04	0.22±0.02	0.17±0.04

Table 3: Results on synthetic dataset.

Feature	RMSE (↓)		Frechet (↓)	
	$\mathcal{N}_{Without}^{Ind}$	\mathcal{N}_{With}^{Ind}	$\mathcal{N}_{Without}^{Ind}$	\mathcal{N}_{With}^{Ind}
W	0.08±0.01	0.04±0.02	0.23±0.02	0.14±0.06
Z	0.06±0.01	0.05±0.00	0.15±0.02	0.13±0.02
X	0.10±0.02	0.10±0.02	0.24±0.03	0.24±0.03
Average	0.08±0.01	0.06±0.01	0.20±0.02	0.17±0.04

Table 4: Ablation study on synthetic dataset.

Auto-MPG: In this experiment, we work on Auto-MPG dataset [7] where the task is to predict *miles per gallon* (MPG) based on various parameters such as *acceleration*, *horsepower*, etc. We do not know the ground truth causal graph in this case. Hence, we first construct a causal graph as shown in Fig 4 based on pertinent domain knowledge. Subsequently, we verify the correctness of this constructed causal graph through interaction with the popular large language model GPT-3.5 [2], questioning the correctness of each causal edge within the constructed graph. We use this constructed graph as the available knowledge in our experiments. Tab 5 shows these results. Since the underlying structural equations are unavailable for this dataset, we cannot evaluate indirect causal effects. However, we can compare the performance with respect to total causal effects, which is the sum of direct and indirect causal effects. From the results, our method outperforms baselines in capturing true total causal effects.

Lung Cancer: In Lung Cancer dataset [39], whose causal graph is known (see Fig 4), we consider *Dyspnea* is the output variable with the remaining features such as *smoking*, *bronchitis*, etc. as inputs. From the results shown in Tab 5, our model is better at learning the true total causal effects when compared to the baselines. The lateral connections among input features are implemented using simple multi-layer perceptrons with non-linear activation functions. Since the underlying causal graph of the Lung Cancer dataset is a discrete Bayesian network with binary-valued features, the Frechet score is not relevant, and so we report only RMSE values for this dataset. Similar to Auto-MPG dataset, we present results on total causal effects. **Sachs:** Sachs dataset consists of 11 protein types and their causal relationships as shown in Fig 4. We consider the variable *Akt* as output and the remaining variables *Plcg*, *PIP2*, *PIP3* as inputs as they do not causally influence the output. The results in Tab 5 show that our model is better at learning the true total causal effects than the baselines.

To check that the second phase of our proposed ante-hoc training algorithm, where we train the parameters of layer 0, does not reduce the model performance, we check the performance on each dataset after each epoch for each training phase. As shown in Fig 5, the two phases of ante-hoc model training converge without oscillations in phase 2 training. **Flight Simulation Datasets:** To study the value of our efficient implementation strategies discussed in Sec. 4.3, we consider flight simulation datasets that benefit from such strategies. We consider three different time series-based datasets: *Parking Brake Dataset (PBD)*, *Flap Dataset (FD)* and *Multiple Anomaly Dataset (MAD)* which simulate the application of parking brakes during the takeoff, the de-

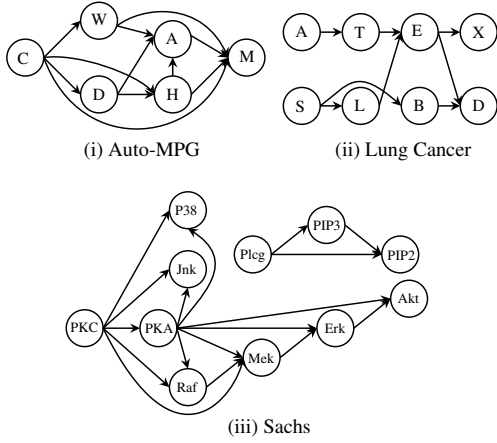


Figure 4: (i) Estimated causal graph of Auto-MPG dataset where C: number of cylinders, D: displacement, W: weight, H: horsepower, A: acceleration, and M: miles per gallon. (ii) True causal graph of lung cancer dataset where A: visit to Asia, T: tuberculosis, S: smoking, L: lung cancer, B: bronchitis, E: either T or L, X: X-ray, and D: dyspnea. (iii) True causal graph of Sachs dataset.

Feature	IG [S 2017]	CA [AC 2019]	CSHAP [TH 2020]	CREDO [SK 2022]	AHCE (Ours)	
Auto-MPG						
RMSE (\downarrow)	Cylinders	0.12±0.00	0.13±0.00	0.20±0.00	0.11±0.02	0.01±0.00
	Disp.	0.11±0.00	0.11±0.00	0.20±0.00	0.09±0.02	0.11±0.01
	Horsepow.	0.21±0.02	0.04±0.01	0.17±0.00	0.07±0.02	0.09±0.01
	Weight	0.27±0.04	0.09±0.00	0.05±0.00	0.09±0.02	0.07±0.00
	Acceler.	0.07±0.01	0.07±0.00	0.02±0.00	0.15±0.05	0.07±0.00
	Average	0.16±0.02	0.09±0.00	0.13±0.00	0.10±0.02	0.07±0.00
Frechet (\downarrow)	Cylinders	0.27±0.00	0.25±0.00	0.37±0.00	0.22±0.04	0.03±0.03
	Disp.	0.25±0.00	0.21±0.01	0.38±0.00	0.19±0.03	0.21±0.02
	Horsepow.	0.25±0.02	0.07±0.02	0.30±0.00	0.15±0.03	0.18±0.03
	Weight	0.45±0.08	0.15±0.02	0.06±0.02	0.17±0.06	0.09±0.01
	Acceler.	0.12±0.01	0.09±0.01	0.06±0.01	0.33±0.16	0.10±0.00
	Average	0.27±0.02	0.16±0.01	0.23±0.00	0.21±0.06	0.12±0.02
Lung Cancer						
RMSE (\downarrow)	Asia	0.46±0.05	0.38±0.11	0.00±0.00	0.00±0.00	0.05±0.06
	Tub.	0.62±0.04	1.13±0.04	0.99±0.00	1.00±0.00	0.58±0.29
	Smoking	1.07±0.07	1.01±0.00	0.99±0.00	1.00±0.00	0.56±0.33
	L.Cancer	0.40±0.07	0.62±0.02	0.48±0.04	0.49±0.00	0.77±0.75
	Bronch.	1.55±0.14	1.48±0.06	0.93±0.00	1.08±0.01	1.11±0.51
	Either	0.87±0.18	0.78±0.06	0.53±0.03	0.55±0.00	0.65±0.23
	X-ray	0.11±0.05	0.09±0.04	0.03±0.00	0.00±0.00	0.08±0.12
	Average	0.72±0.09	0.78±0.05	0.56±0.00	0.59±0.00	0.54±0.33
Sachs						
RMSE (\downarrow)	PKC	0.08±0.07	0.10±0.09	0.19±0.00	0.08±0.02	0.12±0.06
	PKA	2.29±1.40	2.19±0.90	0.46±0.00	3.81±0.02	0.65±0.17
	Raf	0.15±0.03	0.11±0.05	0.24±0.00	0.02±0.02	0.12±0.03
	Mek	0.20±0.04	0.21±0.13	0.23±0.00	0.42±0.02	0.14±0.01
	Erk	4.33±3.25	0.63±2.23	0.53±0.00	2.87±0.05	0.51±0.34
	Jnk	0.08±0.04	0.07±0.04	0.25±0.00	0.13±0.05	0.01±0.01
	P38	0.26±0.18	0.09±0.06	0.31±0.00	0.04±0.05	0.02±0.01
Average	1.05±0.71	0.71±0.27	0.32±0.00	1.05±0.00	0.22±0.09	
Frechet (\downarrow)	PKC	0.14±0.12	0.13±0.12	0.30±0.00	0.11±0.00	0.17±0.09
	PKA	2.89±1.62	2.97±1.14	0.29±0.00	5.02±0.02	0.91±0.23
	Raf	0.21±0.05	0.16±0.08	0.27±0.00	0.03±0.02	0.17±0.05
	Mek	0.33±0.08	0.27±0.18	0.37±0.00	0.56±0.02	0.17±0.01
	Erk	5.63±4.04	3.12±0.90	0.36±0.00	4.04±0.05	0.70±0.45
	Jnk	0.12±0.06	0.09±0.05	0.36±0.00	0.16±0.05	0.02±0.02
	P38	0.41±0.30	0.12±0.09	0.47±0.00	0.06±0.05	0.02±0.02
Average	1.39±0.90	0.98±0.36	0.34±0.00	1.43±0.00	0.31±0.12	

Table 5: Results on Auto-MPG, Lung Cancer, and Sachs datasets

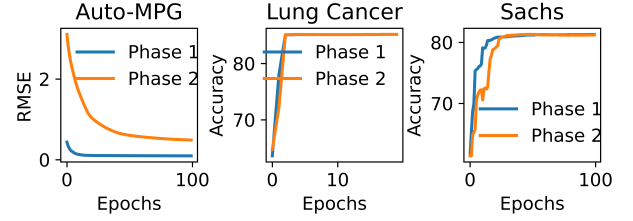


Figure 5: Convergence of RMSE/Accuracy values at the end of two phases of training outlined in Algorithm 1.

Methods(\downarrow)/ Datasets(\rightarrow)	PBD	FD	MAD
CA (Eqn 4)	64.50	69.33	176
CA (Hess.×Cov.)	20	41	91
$\nabla^2 f \approx J^T J$	18.5	24	48.50
Ours + CA	21.50	25.5	73
Ours + CA (Hess.×Cov.)	0.13	20	25
Ours + ($\nabla^2 f \approx J^T J$)	0.004	1	3

Table 6: Time taken in minutes by different methods of finding causal effects for flight simulation datasets.

ployment of a wrong flap during takeoff and the multiple brake anomalies (*left-brake*, *right-brake*, and *auto-brake*) respectively. These datasets are captured on an industry-grade flight simulator. In all these datasets, we train an RNN to predict whether a given sequence is anomalous or not. We compare our method with CA and an approximation to the second-order term in Eqn 4 proposed in [3]. Tab 6 shows the results, highlighting the improvements in time needed to compute ACE in our method. Appendix F contains qualitative results showing the performance of these methods using ACE plots.

6 Conclusions

We present a new perspective to learn and quantify causal effects in NNs. Using available prior causal knowledge, we design an ante-hoc causal explanation method to study both direct and indirect causal effects of inputs on the output of an NN. The work also presents effective approximation strategies to compute causal effects for high-dimensional data. Our experiments on synthetic and real-world data show significant promise of the methodology to elicit direct and indirect causal effects in an NN model.

References

- [1] Alvarez-Melis, D.; and Jaakkola, T. S. 2017. A causal framework for explaining the predictions of black-box sequence-to-sequence models. *arXiv preprint arXiv:1707.01943*.
- [2] Brown, T. B.; Mann, B.; Ryder, N.; Subbiah, M.; Kaplan, J.; Dhariwal, P.; Neelakantan, A.; Shyam, P.; Sastry, G.; Askell, A.; et al. 2020. Language Models are Few-Shot Learners. *arXiv preprint arXiv:2005.14165*.
- [3] Chattopadhyay, A.; Manupriya, P.; Sarkar, A.; and Bal-

- asubramanian, V. N. 2019. Neural Network Attributions: A Causal Perspective. In *ICML*.
- [4] Dandl, S.; Molnar, C.; Binder, M.; and Bischl, B. 2020. Multi-Objective Counterfactual Explanations. In Bäck, T.; Preuss, M.; Deutz, A.; Wang, H.; Doerr, C.; Emmerich, M.; and Trautmann, H., eds., *Parallel Problem Solving from Nature – PPSN XVI*, 448–469. Springer International Publishing.
- [5] Datta, A.; Sen, S.; and Zick, Y. 2016. Algorithmic Transparency via Quantitative Input Influence: Theory and Experiments with Learning Systems. *2016 IEEE Symposium on Security and Privacy (SP)*, 598–617.
- [6] Došilović, F. K.; Brčić, M.; and Hlupić, N. 2018. Explainable artificial intelligence: A survey. In *2018 41st International Convention on Information and Communication Technology, Electronics and Microelectronics (MIPRO)*, 0210–0215.
- [7] Dua, D.; and Graff, C. 2017. UCI Machine Learning Repository.
- [8] Geva, M.; Caciularu, A.; Dar, G.; Roit, P.; Sadde, S.; Shlain, M.; Tamir, B.; and Goldberg, Y. 2022. LM-Debugger: An Interactive Tool for Inspection and Intervention in Transformer-Based Language Models.
- [9] Goyal, A.; Lamb, A.; Hoffmann, J.; Sodhani, S.; Levine, S.; Bengio, Y.; and Schölkopf, B. 2021. Recurrent Independent Mechanisms. In *ICLR*.
- [10] Goyal, Y.; Feder, A.; Shalit, U.; and Kim, B. 2019. Explaining classifiers with causal concept effect (cace). *arXiv preprint arXiv:1907.07165*.
- [11] Goyal, Y.; Wu, Z.; Ernst, J.; Batra, D.; Parikh, D.; and Lee, S. 2019. Counterfactual Visual Explanations. In *ICML*.
- [12] Hendricks, L. A.; Hu, R.; Darrell, T.; and Akata, Z. 2018. Grounding Visual Explanations. *Lecture Notes in Computer Science*, 269–286.
- [13] Heskens, T.; Sijben, E.; Bucur, I. G.; and Claassen, T. 2020. Causal Shapley Values: Exploiting Causal Knowledge to Explain Individual Predictions of Complex Models. In *NeurIPS*.
- [14] Imbens, G. W.; and Rubin, D. B. 2015. *Causal Inference for Statistics, Social, and Biomedical Sciences: An Introduction*. Cambridge University Press.
- [15] Janzing, D. 2019. Causal regularization. In *NeurIPS*.
- [16] Janzing, D.; Minorics, L.; and Bloebaum, P. 2020. Feature relevance quantification in explainable AI: A causal problem. In *AISTATS*.
- [17] Kancheti, S. S.; Reddy, A. G.; Balasubramanian, V. N.; and Sharma, A. 2022. Matching Learned Causal Effects of Neural Networks with Domain Priors. In *ICML*.
- [18] Khademi, A.; and Honavar, V. 2020. A Causal Lens for Peeking into Black Box Predictive Models: Predictive Model Interpretation via Causal Attribution. *arXiv 2008.00357*.
- [19] Kocaoglu, M.; Snyder, C.; Dimakis, A. G.; and Vishwanath, S. 2018. CausalGAN: Learning Causal Implicit Generative Models with Adversarial Training. In *ICLR*.
- [20] Koh, P. W.; Nguyen, T.; Tang, Y. S.; Musmann, S.; Pierson, E.; Kim, B.; and Liang, P. 2020. Concept Bottleneck Models. *International Conference on Machine Learning*, 5338–5348.
- [21] Kyono, T.; Zhang, Y.; and van der Schaar, M. 2020. CASTLE: Regularization via Auxiliary Causal Graph Discovery. In *NeurIPS*.
- [22] Lundberg, S. M.; and Lee, S.-I. 2017. A Unified Approach to Interpreting Model Predictions. In Guyon, I.; Luxburg, U. V.; Bengio, S.; Wallach, H.; Fergus, R.; Vishwanathan, S.; and Garnett, R., eds., *NIPS*.
- [23] Mahajan, D.; Tan, C.; and Sharma, A. 2019. Preserving Causal Constraints in Counterfactual Explanations for Machine Learning Classifiers. In *CausalML: Machine Learning and Causal Inference for Improved Decision Making Workshop, NeurIPS 2019*.
- [24] Montavon, G.; Lapuschkin, S.; Binder, A.; Samek, W.; and Müller, K.-R. 2017. Explaining nonlinear classification decisions with deep Taylor decomposition. *Pattern Recognition*, 65: 211–222.
- [25] Mothilal, R. K.; Mahajan, D.; Tan, C.; and Sharma, A. 2021. Towards Unifying Feature Attribution and Counterfactual Explanations: Different Means to the Same End. In *AIES*.
- [26] O’Shaughnessy, M.; Canal, G.; Connor, M.; Rozell, C.; and Davenport, M. 2020. Generative causal explanations of black-box classifiers. In *NeurIPS*.
- [27] Parascandolo, G.; Kilbertus, N.; Rojas-Carulla, M.; and Schölkopf, B. 2018. Learning independent causal mechanisms. In *ICML*.
- [28] Pawlowski, N.; Coelho de Castro, D.; and Glocker, B. 2020. Deep Structural Causal Models for Tractable Counterfactual Inference. In *NeurIPS*.
- [29] Pearl, J. 2001. Direct and indirect effects. In *UAI*.
- [30] Pearl, J. 2009. *Causality*. Cambridge university press.
- [31] Ribeiro, M. T.; Singh, S.; and Guestrin, C. 2016. Why should i trust you?: Explaining the predictions of any classifier. In *Proceedings of the 22nd ACM SIGKDD International Conference on Knowledge Discovery and Data Mining*, 1135–1144. ACM.
- [32] Rieger, L.; Singh, C.; Murdoch, W.; and Yu, B. 2020. Interpretations are Useful: Penalizing Explanations to Align Neural Networks with Prior Knowledge. In *ICML*.
- [33] Ross, A. S.; Hughes, M. C.; and Doshi-Velez, F. 2017. Right for the Right Reasons: Training Differentiable Models by Constraining their Explanations. In *IJCAI*, 2662–2670.
- [34] Rudin, C.; Chen, C.; Chen, Z.; Huang, H.; Semenova, L.; and Zhong, C. 2021. Interpretable Machine Learning: Fundamental Principles and 10 Grand Challenges. *Statistics Surveys*.

- [35] Sayres, R.; Kim, B.; Wattenberg, M.; Gilmer, J.; Cai, C.; Wexler, J.; and Viegas, F. 2018. Interpretability Beyond Feature Attribution: Quantitative Testing with Concept Activation Vectors (TCAV). In *Proceedings of the 35th International Conference on Machine Learning*, 2668–2677. PMLR.
- [36] Schölkopf, B.; Locatello, F.; Bauer, S.; Ke, N. R.; Kalchbrenner, N.; Goyal, A.; and Bengio, Y. 2021. Toward causal representation learning. *Proceedings of the IEEE*, 109(5): 612–634.
- [37] Schwab, P.; and Karlen, W. 2019. CXPlain: Causal Explanations for Model Interpretation under Uncertainty. In *NeurIPS*.
- [38] Schwab, P.; Linhardt, L.; Bauer, S.; Buhmann, J. M.; and Karlen, W. 2020. Learning counterfactual representations for estimating individual dose-response curves. In *AAAI*.
- [39] Scutari, M.; and Denis, J. 2014. *Bayesian Networks: With Examples in R*. Chapman & Hall/CRC Texts in Statistical Science. Taylor & Francis.
- [40] Selvaraju, R. R.; Das, A.; Vedantam, R.; Cogswell, M.; Parikh, D.; and Batra, D. 2016. Grad-CAM: Why did you say that? *arXiv preprint arXiv:1611.07450*.
- [41] Shalit, U.; Johansson, F. D.; and Sontag, D. 2017. Estimating individual treatment effect: generalization bounds and algorithms. In *ICML*.
- [42] Simonyan, K.; Vedaldi, A.; and Zisserman, A. 2013. Deep inside convolutional networks: Visualising image classification models and saliency maps. *arXiv preprint arXiv:1312.6034*.
- [43] Smilkov, D.; Thorat, N.; Kim, B.; Viégas, F.; and Wattenberg, M. 2017. Smoothgrad: removing noise by adding noise. *arXiv preprint arXiv:1706.03825*.
- [44] Sundararajan, M.; Taly, A.; and Yan, Q. 2017. Axiomatic Attribution for Deep Networks. In *ICML*.
- [45] Van Looveren, A.; and Klaise, J. 2021. Interpretable Counterfactual Explanations Guided by Prototypes. In Oliver, N.; Pérez-Cruz, F.; Kramer, S.; Read, J.; and Lozano, J. A., eds., *Machine Learning and Knowledge Discovery in Databases. Research Track*, 650–665. Cham: Springer International Publishing.
- [46] Verma, S.; Boonsanong, V.; Hoang, M.; Hines, K. E.; Dickerson, J. P.; and Shah, C. 2020. Counterfactual Explanations and Algorithmic Recourses for Machine Learning: A Review.
- [47] Vig, J.; Gehrmann, S.; Belinkov, Y.; Qian, S.; Nevo, D.; Singer, Y.; and Shieber, S. 2020. Investigating Gender Bias in Language Models Using Causal Mediation Analysis. In *NeurIPS*.
- [48] Wachter, S.; Mittelstadt, B.; and Russell, C. 2018. Counterfactual Explanations Without Opening the Black Box: Automated Decisions and the GDPR. *Harvard journal of law and technology*, 31: 841–887.
- [49] Wang, Y.; Liu, F.; Chen, Z.; Lian, Q.; Hu, S.; Hao, J.; and Wu, Y.-C. 2021. Contrastive ACE: Domain Generalization Through Alignment of Causal Mechanisms. *arXiv 2106.00925*.
- [50] Wickramanayake, S.; Hsu, W.; and Lee, M. L. 2019. FLEX: Faithful Linguistic Explanations for Neural Net Based Model Decisions. In *Proceedings of the AAAI Conference on Artificial Intelligence*, 2539–2546. AAAI.
- [51] Wickramanayake, S.; Hsu, W.; and Lee, M. L. 2021. Comprehensible Convolutional Neural Networks via Guided Concept Learning. In *2021 International Joint Conference on Neural Networks (IJCNN)*, 1–8.
- [52] Xia, K.; Lee, K.-Z.; Bengio, Y.; and Bareinboim, E. 2021. The causal-neural connection: Expressiveness, learnability, and inference. *NeurIPS*.
- [53] Yadu, A.; Suhas, P. K.; and Sinha, N. 2021. Class Specific Interpretability in CNN Using Causal Analysis. In *2021 IEEE International Conference on Image Processing (ICIP)*, 3702–3706.
- [54] Zarlenga, M. E.; Barbiero, P.; Ciravegna, G.; Marra, G.; Giannini, F.; Diligenti, M.; Shams, Z.; Precioso, F.; Melacci, S.; Weller, A.; Lio, P.; and Jamnik, M. 2022. Concept Embedding Models: Beyond the Accuracy-Explainability Trade-Off. *arXiv preprint arXiv:2209.09056*.
- [55] Zeiler, M. D.; and Fergus, R. 2014. Visualizing and understanding convolutional networks. In *ECCV*, 818–833. Springer.
- [56] Zhang, W.; Liu, L.; and Li, J. 2021. Treatment Effect Estimation with Disentangled Latent Factors. In *AAAI*.
- [57] Zhou, B.; Sun, Y.; Bau, D.; and Torralba, A. 2018. Interpretable Basis Decomposition for Visual Explanation. In *ECCV*. Springer.

Appendix

In this Appendix, we include the following additional information, which we could not include in the main paper due to space constraints.

- Causality preliminaries are presented in § A.
- Comparison of our method with causal Shapley values is presented in § B
- Proof of causal effect identifiability is given in § C.
- Algorithm for evaluating direct and indirect causal effects in NNs and an algorithm for efficient implementation using the binning approach are outlined in § D.
- Experimental setup and additional results are in § E.
- Details on efficient implementation strategies are presented in § F.
- Related work on concept-based explainability is discussed in § G.
- A motivating example for learning and explaining indirect causal effects is given in § H.
- Uniqueness and usefulness of causal explanations is discussed in § I.

A Causality Preliminaries

This section provides the basic definitions and concepts required to understand our paper. We start with two popular ways of modeling causality in the real world: (i) structural causal models and (ii) causal graphical models.

Structural Causal Models: A Structural Causal Model (SCM) $\mathcal{S}(\mathbf{V}, \mathbf{U}, \mathcal{F}, P_{\mathbf{U}})$ encodes cause-effect relationships among a set of random variables $\mathbf{V} \cup \mathbf{U}$ using a set of structural equations \mathcal{F} relating each variable $X \in \mathbf{V} \cup \mathbf{U}$ with its parents $pa(X) \in \mathbf{V} \cup \mathbf{U} \setminus \{X\}$. That is, each variable $X \in \mathbf{V}$ is obtained using the structural equation as $X = f(pa(X))$ for some $f \in \mathcal{F}$. The variables in \mathbf{U} are called exogenous variables denoting uncontrolled external factors. $P_{\mathbf{U}}$ is the probability distribution of exogenous variables. The variables in \mathbf{V} are called endogenous variables.

Causal Graphical Models: A causal graphical model $\mathcal{G}(\mathbf{V} \cup \mathbf{U}, \mathcal{E})$ consists of a set of vertices $\mathbf{V} \cup \mathbf{U}$ and a set of edges \mathcal{E} . The set of edges \mathcal{E} indicate the causal relationships among the variables in $\mathbf{V} \cup \mathbf{U}$. To make an analogy between structural causal models and causal graphical models, the set of vertices \mathbf{V} corresponds to the set of endogenous variables, the set of vertices \mathbf{U} corresponds to the set of exogenous variables, and the set of edges \mathcal{E} corresponds to the set of structural equations \mathcal{F} relating each variable with its parents. Concretely, if $X = f(pa(X)); f \in \mathcal{F}$, then $\forall X_i \in pa(X)$, we draw a directed edge from X_i to X . A *path* in a causal graph is defined as a sequence of unique vertices X_1, X_2, \dots, X_n with an edge between each consecutive vertices X_i and X_{i+1} where the edge between X_i and X_{i+1} can be either $X_i \rightarrow X_{i+1}$ or $X_{i+1} \rightarrow X_i$. A *directed path* is defined as a sequence of unique vertices X_1, X_2, \dots, X_n with an edge between each consecutive vertices X_i and X_{i+1} so that the edge between X_i and X_{i+1} takes the form $X_i \rightarrow X_{i+1}$. If there exists a directed path from X_i to X_j , X_i is called an ancestor of X_j and X_j is called a descendant of X_i .

There are three basic causal structures formed with three variables $X_1, X_2, X_3 \in \mathbf{V}$: (1) $X_1 \rightarrow X_2 \rightarrow X_3$, (2) $X_1 \leftarrow X_2 \rightarrow X_3$, (3) $X_1 \rightarrow X_2 \leftarrow X_3$. These three basic causal structures are called *chain*, *fork*, and *collider*, respectively. X_2 in $X_1 \rightarrow X_2 \leftarrow X_3$ is called collider node. X_1, X_2, X_3 form a *v-structure* in \mathcal{G} if they form a collider structure $X_1 \rightarrow X_2 \leftarrow X_3$ with X_1, X_3 being non-adjacent. A *backdoor* path from X_i to X_j is a path that starts with an arrow into X_i (i.e., a path that starts with $X_i \leftarrow$). A directed path starting from a node X_i and ending at a node X_j is called a *causal path* from X_i to X_j . A path that is not a causal path is called a *non-causal path*. For example, the path $X_1 \rightarrow X_2 \rightarrow X_3$ is a causal path from X_1 to X_3 , and the path $X_1 \leftarrow X_2 \rightarrow X_3$ is a non-causal path from X_1 to X_3 . The causal effect of a variable X_i on another variable X_j that is not flowing through other variables is known as the direct causal effect. The causal effect of a variable X_i on another variable X_j flowing through other variables is known as the indirect causal effect. For example, consider Fig A1. The causal effect of X_1 on X_3 that flows through the causal path $X_1 \rightarrow X_3$ is the direct causal effect, and the causal effect of X_1 on X_3 that flows through the causal path $X_1 \rightarrow X_2 \rightarrow X_3$ is the indirect causal effect.

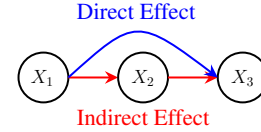


Figure A1: Direct and indirect effects of X_1 on X_3 .

Definition A.1. (*d-Separation*.) A path p between X_i and X_j given $\mathbf{S} \subset \mathbf{V} \setminus \{X_i, X_j\}$ is said to be open, if and only if (1) every collider node on p is in \mathbf{S} or has a descendant in \mathbf{S} , and (2) no other non-collider variables on p are in \mathbf{S} . If the path p is not open, then p is blocked. X_i and X_j are *d-separated* given \mathbf{S} , if and only if every path from X_i to X_j is blocked by \mathbf{S} .

Definition A.2. (*The Backdoor Criterion*.) Given a pair of variables $(X_i, X_j) \in \mathbf{V} \times \mathbf{V}$, a set of variables $\mathbf{S} \subset \mathbf{V}$ satisfies the backdoor criterion relative to (X_i, X_j) if no node in \mathbf{S} is a descendant of X_i , and \mathbf{S} blocks every backdoor path between X_i and X_j .

Definition A.3. (*Interventional Distribution* [30].) The interventional distribution of a set of variables $\mathbf{X} = \{X_1, \dots, X_n\}$ under an intervention to X_i with a value x_i , denoted by $do(X_i = x_i)$, is defined as follows.

$$p(\mathbf{X} | do(X_i = x_i)) = \begin{cases} \prod_{j \neq i} p(X_j | pa(X_j)) & \text{if } X_i = x_i \\ 0 & \text{if } X_i \neq x_i \end{cases}$$

The resulting probability distribution of a set of variables $\mathbf{X}_{\setminus i} = \{X_1, \dots, X_n\} \setminus \{X_i\}$ under the intervention $do(X_i = x_i)$ is same as the probability distribution of $\mathbf{X}_{\setminus i}$ induced by the *intervened/manipulated* causal graph $\mathcal{G}_{do(X_i)} \cdot \mathcal{G}_{do(X_i)}$ is obtained by removing all incoming arrows to X_i in \mathcal{G} [30].

Dataset	Num. of Features	Num. Data Points	Architecture	Application	Algorithms Studied
Synthetic data	3	1000	Feedforward neural network	Regression	1, 2
AutoMPG	5	392	Feedforward neural network	Regression	1, 2
Lung Cancer	7	10,000	Feedforward neural network	Classification	1, 2
SACHS	11	10,000	Feedforward neural network	Classification	1, 2
Parking brake	48	3360	Recurrent neural network	Classification	3
Flap	96	6370	Recurrent neural network	Classification	3
Multiple anomaly	52	4403	Recurrent neural network	Classification	3

Table A1: Summary of datasets and applications

for \mathcal{N}^{Ind} . Algorithm 3 outlines the binning methodology to improve the run time requirements to find causal effects.

Algorithm 3: Pseudocode for efficient evaluation of $ACE_{X_i}^{\hat{Y}}$

```

1: Input: Test sample  $\mathbf{X}_{te}, X_i$ , Intervention value  $\alpha$ , Database
    $DB$  to store offline interventional statistics, Training data  $\mathcal{D}$ ,
   Nearest neighbor function  $NB$ .
2: Output:  $\mathbb{E}[\hat{Y}|do(X_i = \alpha)]$ 
3: \* Offline Phase * \
4: for  $\mathbf{X}_{tr} \in \mathcal{D}$  do
5:    $DB[\mathbf{X}_{tr}; E; x_i] = \mathbb{E}[X_j|do(X_i)] \forall j, x_i$ 
6:    $DB[\mathbf{X}_{tr}; C; x_i] = Covariance(X_j, X_l|do(X_i)) \forall j, l, x_i$ 
7: end for
8: \* Online Phase * \
9: step 1:  $\mathbf{X}_{tr} = NB(\mathbf{X}_{te}, \mathcal{D})$ 
10: step 2:  $x_i = NB(\beta)$ 
11: step 3:  $\mathbb{E}[X_j|do(X_i)] \forall j = DB[\mathbf{X}_{tr}; E; x_i]$ 
12: step 4:  $Cov(X_j, X_l|do(X_i)) \forall j, l = DB[\mathbf{X}_{tr}; C; x_i]$ 
13: step 5: Evaluate  $ACE_{X_i}^{\hat{Y}}$  using  $\mathbb{E}[X_j|do(X_i)] \forall j,$ 
    $Covariance(X_j, X_l|do(X_i)) \forall j, l$ 
14: return  $ACE_{X_i}^{\hat{Y}}$ 

```

E Experimental Setup and Additional Results

In this section, we present details on the experimental setup. Tab A1 shows the details on the datasets and applications we study in this paper. In the Sachs dataset, we compute causal effects of inputs on the first output neuron among three neurons in the final layer. Integrated Gradients (IG), Causal Attributions (CA), and Causal Shapley (CSHAP) explanations are obtained on a model trained with empirical risk minimization loss (ERM). Apart from ERM, we train CREDO, a causal regularization method, and our proposed AHCE method. From the results in the main paper, the proposed AHCE method gives better causal explanations than baselines with no change in downstream performance. Tab A2 supports the fact that there is no significant difference in the performance of the three models: ERM, CREDO, and AHCE. If an input feature is real-valued, we consider 1000 interventions (i.e., 1000 X_i values in Eqn 4) in its input range to calculate interventional expectation values. Across all our experiments, we use Adam optimizer with default parameter values except for weight decay, which we set to 0.0001. Batch sizes for the Synthetic, Auto-MPG, Lung

Dataset(→) Method(↓)	Synthetic (RMSE (↓))	Auto-MPG (RMSE (↓))	Lung Cancer (Accuracy (↑))	Sachs (Accuracy (↑))
ERM	0.008±0.00	0.008±0.00	85.09±0.00	81.55±0.18
CREDO	0.012±0.00	0.016±0.00	84.09±0.03	81.69±0.00
AHCE	0.010±0.00	0.013±0.00	85.09±0.00	81.45±0.02

Table A2: Performance of methods on various datasets.

	Feature	CSHAP [TH 2020]	AHCE (Ours)
RMSE (↓)	W	3.26±0.00	3.09±0.00
	Z	1.82±0.00	1.89±0.00
	X	0.09±0.00	0.02±0.00
	Average	1.72±0.00	1.67±0.01
Frechet (↓)	W	4.52±0.00	4.74±0.05
	Z	3.71±0.00	3.81±0.00
	X	0.16±0.00	0.04±0.04
	Average	2.80±0.00	2.86±0.03

Table A3: Comparison of CSHAP and AHCE w.r.t. indirect causal effects on synthetic dataset.

Cancer, and Sachs experiments are 1, 1, 16, and 64, respectively. We get the best results with 20 training epochs for experiments performed on Synthetic and AutoMPG datasets, whereas we observe that 50 epochs are required in the case of SACHS and Lung Cancer to obtain good results. For the Integrated Gradients method (IG), we set the n_steps parameter to be 50 across all experiments. Since obtaining Shapley values is computationally expensive, we pick 100 values randomly from the dataset to compute them and subsequently calculate the performance metrics (we observe that the number of data points has a minor impact on the overall Shapley values).

The main paper contains results w.r.t. total causal effects. We present the results w.r.t. indirect causal effects in Tab A3. As noted in the main paper § 5, the indirect effects do not exist for IG, CA, and CREDO. For real-world datasets, we do not have access to the underlying structural equations; hence, we cannot evaluate ground truth indirect causal effects. Figure A2 shows the absolute ACE values of each feature at different time steps for three time-series datasets and baseline methods. In Fig A2, ‘Exact’ method refers to the evaluation of Eqn 4, ‘Approx’ method refers to the approximation to the second order term in Eqn 4 proposed in [3], ‘Newtonian’ method refers to the Newtonian approximation $\nabla^2 f \approx J^T J$. For each plot in Fig A2, x-axis denotes the



Figure A2: Results on binning approximation to causal explanations for time series data

time step (unrolling length of RNN), and y-axis denotes the features. It can be seen that, in many cases, the proposed approximation’s causal explanations (last four columns) are close to the exact computation of causal explanations (first two columns). However, there is a trade-off between the binning parameters (number of bins, distance function used in clustering methods, etc.) and the obtained causal explanations.

F Efficient Implementation Strategies

In this section, we expound on the strategies to reduce the storage requirements for binning approach (Sec 4.3 of main paper). The overall approach of online-offline (binning) method is outlined in Figure A3. Storing offline interventional statistics for every point on the dataset becomes impractical. This is owing to the multiple aspects of data at each time step of computing interventional expectation: the number of interventional values, the number of features, and in the case of RNNs, the unrolling length of RNN. Even if storage bottlenecks are not a concern, managing a data structure that can address, log, and access this on-demand becomes tedious and counter-intuitive. So we seek to reduce the number of points, the number of interventions for each point, and the amount of data stored per point while maintaining the accuracy of online results of incoming points.

We get data clusters so that the cluster centers can be used as a proxy for cluster points so that the number of points to compare with a test data point during the online phase are significantly less. However, the success of clustering methods differs greatly owing to many factors. One important consideration is the distance function used. Euclidean dis-

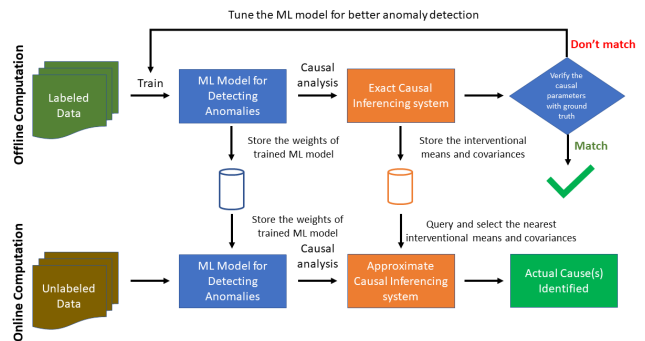


Figure A3: Binnig (offline - online) framework for quick and accurate explainability

tances are standard and, owing to current experimental hurdles, are used herein experiments. But ideally, a distance metric that depends on the accuracy of the ACE values (entire pipeline from offline to online) is ideal. We seek to find clustering methods on the dataset with a minimum accuracy trade-off while maximizing the number of points clustered, thus reducing storage by the average size of the cluster. We use the following clustering methods in this work.

KD Tree: A K-Dimensional (KD) tree is constructed with flattened points so that cluster centroids can be extracted and used for offline computation. Here a hyperparameter is the maximum distance between two points for them to be considered neighbors. Our experiments suggest a Euclidean distance of 10 is ideal, but a roll-off till 20 is still acceptable.

DBSCAN: Since the nature and shape of the clusters are unknown, we can use DBSCAN to get a density-based estimate, where points too sparsely connected to an existing cluster would be considered as outliers. This adds another hyperparameter apart from the maximum distance, called minimum points, that quantifies the number of nearby points needed to consider it as a cluster. This allows us to have a handle on the storage requirements but setting this value too high results in many points being outliers without a cluster.

Complexity Analysis in RNNs In RNNs, the number of steps to unroll the network, call the *chunk* size, impacts the dataset size when we collect data from a stream. From a data stream, we split the dataset such that chunks are overlapping sub-sequences i.e., if the length of a stream is l and chunk size is k , we get approximately $l - k$ chunks in total. Evaluating Eqn 3 takes order of $\mathcal{O}(l \times n^p)$ time (assuming $k \ll l$ and features are p -valued, n is the of input size). On the other hand, evaluating the approximation in Eqn 4 also scales in the order of $\mathcal{O}(kn)$ as the inputs at a particular time step affect the inputs at the next time step in RNNs. In RNNs, interventional statistics calculation takes considerable time as these steps have to be done for every feature in the data point at every time step starting from t to 1, where t is the time step at which we wish to calculate the causal effect, which would take considerable time.

G Related Work on Concept-Based Explanations

Concept-based explanation models attempt to explain an NN model behavior in terms of semantically meaningful concepts in the input when the input is not readily expressed as a discrete set of concepts. Concept bottleneck models [20], and concept embedding models [54] learn the relationship between manually annotated concepts in the input samples and the model predictions. Linguistic concept-based explanation models, such as [50, 51] try to automatically discover semantically meaningful concepts in the input space by leveraging text annotations corresponding to the inputs and using them to explain model predictions. Quantitative testing with concept activation vectors (TCAV) [35] can be used as a post hoc method to explain model predictions in terms of arbitrary concepts that may exist in the input samples but are not known at the time of training. [57] is a method to decompose the input samples into semantically interpretable concepts derived from a pre-trained concept corpus. However, as discussed earlier, when the number of concepts is more, evaluating the causal explanations is time-consuming. In this work, we tackle this time complexity issue using the binning approach as explained in Sec 4.3 and in Appendix § F.

H Motivating Example for Modeling Indirect Causal Effects

Besides the illustrative example presented in section § 1 of the main paper, this section introduces another motivating example that underscores the importance of contemplating indirect causal effects within an NN model.

Consider predicting the health condition H of a patient using their age A and consumed medicine dose M . In the real-world, the age group may determine the medicine dosage value to administer, i.e., $A \rightarrow M$ (e.g., adults are administered higher dosages as compared to children). Also, A and M have direct causal effects on H . That is $A \rightarrow H, M \rightarrow H$. However, in a simple feed-forward NN, we do not have $A \rightarrow M$. If we train an ante-hoc model by adding the edge $A \rightarrow M$ to the NN, we can study the indirect effects of A on H . In this case, it is desirable for A to have non-zero direct and indirect causal effects on the output. If any one of the direct or indirect causal effects of A on H is zero or very small in magnitude, we can conclude that the model has not learned correct relationships. We can then use our explanations to study data biases or to debug the model for potential improvement of model performance while maintaining real-world causal relationships in the NN model.

I Uniqueness and Usefulness of Causal Explanations

In this section, we discuss how causal explanations are different and much more useful when compared to any other explanations in safety-critical applications. Consider the example of a clinical decision support application. When an NN model is used to predict the *risk of cardiac disease*, a

high importance for an input variable such as *hypertension* may arise due to its high correlation with *risk of cardiac disease*. However, the person's *diet choice* (another input variable) may be causing both *hypertension* and *risk of cardiac disease*. Modeling and studying causal effects in NN models help a medical practitioner take appropriate decisions, compared to the reliance on non-causal explanations.